THE MECHANISM BEHIND Pd(II) AND CARBOFURAN-INDUCED CHANGE OF GRAPHENE QUANTUM DOTS PHOTOLUMINESCENCE INTENSITY

Slađana Dorontić[1], Dušan Sredojević[1], Danica Bajuk-Bogdanović[2], Svetlana Jovanović[1]

[1]Vinča Institute of Nuclear Sciences - National Institute of the Republic of Serbia, University of Belgrade P.O. Box 522, 11001 Belgrade, Serbia
[2]Faculty of Physical Chemistry, University of Belgrade, P.O. Box 47, 11158 Belgrade, Serbia
e-mail: sladjana.dorontic@vin.bg.ac.rs

Abstract
The increasing presence of pesticides and heavy metals in the environment and their negative impact on human, animal, and plant health, demand green, low-cost, and simple methods for their monitoring. Due to photoluminescence (PL) in the visible part of the spectrum, biocompatibility, and ecological acceptability, graphene quantum dots (GQDs) are at the center of attention in the field of optical sensing. GQDs show great potential as PL sensors for Pd(II) ions and insecticide carbofuran. In this work, FTIR spectroscopy and Density Functional Theory (DFT) calculation were used to resolve the mechanism of PL change in the presence of these analytes.

Introduction
Among the many hazardous compounds present in the environment, heavy metals and pesticides are the most common pollutants. Due to high toxicity, they have harmful effects on human health, ecosystems, food, as well as drinkable water [1]. For a long time, the insecticide carbofuran (CF) was the most frequently used in crop protection against insects to improve their yield and quality [2]. The United States Environment Protection Agency (US EPA) has completely banned its application in any form [3]. Apart from agriculture, the pharmaceutical, and metal industry also contribute to global pollution. Palladium was found as an excellent catalytic agent in organic chemistry and drug production. Residues of this element in final products reach the environment causing damage [1].
One of the latest discovered members of carbon nanomaterials, graphene quantum dots (GQDs) found an important place in many scientific fields such as energy storage and conversion [4], bioimaging, photodynamic therapy, as well as antioxidative agents [5]. They are 0D nanoparticles less than 100 nm, with an sp^2 graphene core where different oxygen-contained moieties are bounded [2]. Their remarkable properties such as water solubility, biocompatibility, non-toxicity, PL in the visible part of the spectrum, as well as photostability make them a promising candidate for application in the optical detection of pesticides and heavy metals [1].
In this paper, GQDs were produced in the eco-friendly single-step top-down electrochemical oxidation of graphite electrodes. To improve their optical properties, they were gamma-irradiated at a dose of 200 kGy in the presence of 1g ethylenediamine (EDA). In earlier research, these dots were tested as PL probes for the detection of Pd(II) and CF [1, 2]. Now, we resolved the mechanism of the Pd(II) and CF-induced fluorescence change of GQDs using infrared spectroscopy with Fourier transformation (FTIR) and Density Functional Theory (DFT) calculations.

Experimental

GQDs were fabricated by the previously described method [6]. For gamma irradiation, water dispersion of GQDs in the concentration of 1 mg mL^{-1} was mixed with 1g of EDA. To remove molecular oxygen before irradiation, the mixture was bubbled with Ar. The sample was irradiated at a dose of 200 kGy. As a radioactive source, a ^{60}Co was used. Irradiated dots were labeled as γGQDs.

The morphology of γGQDs was analyzed using Quesant AFM (Agoura Hills, CA, USA). Structural characterization of γGQDs was performed at FTIR spectrometer (Thermo Nicolet iS20, Waltham, Massachusetts, MA, USA). PL spectra of γGQDs at different excitation wavelengths in the range of 300-400 nm were recorded at HORIBA Jobin Yvon's Fluoromax-4 spectrometer (Horiba, Kyoto, Japan). UV-Vis spectra were recorded using LLG-uniSPEC 2 Spectrophotometer (Lab Logistic Group, Meckenheim, Germany). For FTIR spectroscopy, $PdCl_2$ and CF solutions were mixed with GQDs and dried into powder. Powdered samples were mixed with KBr and compressed into pellets.

All DFT calculations were performed by using the Gaussian 09 suite of programs [7]. The $C_{60}O_{19}N_3H_{25}$ cluster, with 19 hexagonal C_6-rings, was employed as a model system for the DFT calculations to examine the electronic structure and adsorption properties of N-dopped GQD. The ground-state geometry optimization of bare GQD, GQD/Pd(II), and GQD···CF structures were carried out in the aqueous phase, including the SMD solvent model [8] using the B3LYP hybrid functional [9, 10] The LANL2DZ small-core ECP (effective core potential) basis set [11] was used for Pd(II) ions, in which 28 core electrons are exchanged by an effective potential, and the remaining 16 electrons occupy the valence space, while the Pople's valence double-ζ polarized 6-31G(d,p) basis set [12] was chosen for the light atoms. The frequency calculations were performed at the same level of theory to prove that the optimized structures present true minima and to estimate the Gibbs free energies of adsorption in an aqueous solution. The optimized geometries of the clusters, ESP maps, and NBO color schemes were obtained by the GaussView software [13], while the total density of state diagram (TDOS) was derived from the GaussSum program [14].

Results and discussion

Characterization of GQDs

In Fig. 1a, a 3D AFM image of γGQDs is presented and shows that dots are well-dispersed nanoparticles. Their heights vary from 0.5-5 nm which correspond to 3-5 graphene layers. In the FTIR spectrum of the sample (Fig. 1b), bands in the region 3420-3250 cm^{-1} are assigned to stretching vibration of O-H and N-H bonds in hydroxyl and amino groups, respectively.

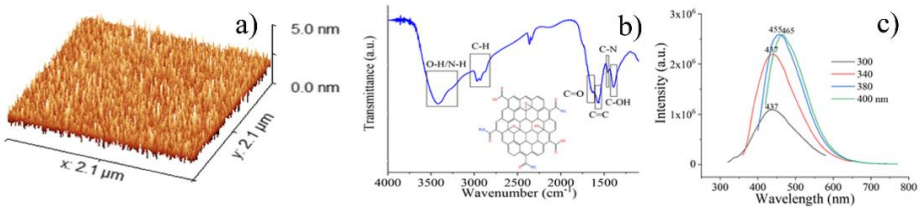

Fig. 1. a) 3D AFM image, b) FTIR spectrum with the schematic presentation of the structure, and c) PL spectra of γGQDs recorded at excitation wavelength 300-400 nm.

The weak band around 1700 cm^{-1} is attributed to stretching C=O vibrations in carboxyl moieties, while bands in region 2870-2970 confirmed the presence of C-H bonds in -CH, and -CH_2 functional groups. Band at 1570 cm^{-1}, verified the presence of graphene structure. The band detected at 1460 cm^{-1} is attributed to the C-N bending vibration of the amide functional group [2].

FTIR spectroscopy confirmed the successful incorporation of N atoms in GQDs structure in form of amide and amino functional groups. PL spectra of γGQDs (Fig. 1c) show that these dots emit light in a blue part of the spectrum, and exhibit excitation-depended PL. With the increase of the excitation wavelength, the center of the emission peak was shifted from 437 to 465 nm.

Mechanism of Pd^{2+} and CF detection

In previous investigations, we examine GQDs with amine and amide groups as PL probes for Pd(II) and CF [1, 2]. We found a linear decrease of GQDs PL intensity in the presence of Pd(II) in the concentration range 0-7.5 μmol L^{-1} with a limit of detection (LOD) of 0.66 μmol L^{-1}[1]. On the contrary, CF led to a linear enhancement of PL intensity in the range of 15-100 μmol L^{-1}, where LOD was 5.4 μmol L^{-1}[2]. The mechanism behind Pd^{2+} and CF detection was investigated using FTIR spectroscopy and DFT analysis.

In Fig. 2a FTIR spectrum of the γGQDs-Pd(II) system is presented. The band at 3420 and at 1700 are slightly reduced and moved to 3422 and 1712 cm^{-1} due to complexation between hydroxyl and carboxyl functional groups at GQDs surface and Pd(II) ions. The shift of band at 1570 attributed to stretching vibrations of C=C bonds in π-conjugated domains, to 1635 cm^{-1} indicates the transfer of GQDs π-electrons to unfilled d orbitals of Pd(II) ions [2]. In UV-Vis spectra of untreated γGQDs-200kGy (Fig. 2b, black curve) absorption bands at 200, and 250 nm are attributed to π-π* transition in sp^2 domains, and n-π* transition in C=O functional groups. After the addition of Pd(II) ions (Fig. 2b, red curve) in the system, bands at 200 and 250 nm, are becoming more pronounced and shifted to 239 and 279 nm, due to cation-π interactions and complex formation, respectively. [1].

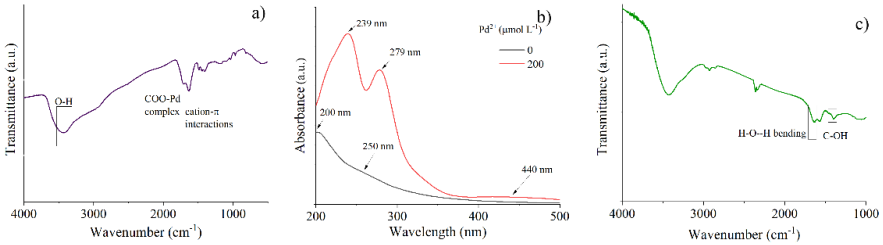

Fig. 2. a) FTIR and b) UV-Vis spectra of γGQDs in the presence of Pd(II) ions, and FTIR spectra of γGQDs in the presence of CF.

A compared with FTIR spectra of pure γGQDs (Fig. 1b) FTIR spectra of γGQDs-CF system also some changes can be noticed (Fig. 2c). Band arround 1700 cm^{-1} became more pronounced due to bending vibration of H-bonds formed between carboxyl group on GQDs surface and CF. [2].

DFT analysis

To investigate the mechanism of the Pd(II) induced fluorescence quenching of γGQDs, we employed DFT calculations to elucidate the interactions between Pd(II) ions with different parts of the GQD molecule at the atomistic level. On the other side, we estimated the energy of hydrogen bonding between carbofuran molecules with GQDs, which led to enhanced photoluminescence intensity due to the structural rigidification of GQD particles. The density of state diagram (DOS) with the spatial distribution of frontier molecular orbitals (FMOs), the optimized structure of GQD, and the electrostatic potential map of GQD molecule are presented in Fig. 3. The valence band maximum (VBM) and conduction band minimum (CBM) approximated with HOMO/LUMO orbitals of the GQD cluster are located at −5.53 and −2.98 eV, respectively (Fig. 3a). These values determine the HOMO-LUMO gap of 2.55 eV, which

is comparable with the experimentally measured absorption onset of the GQDs (~400 nm; 3 eV). The optimized structure of GQD reveals that the planarity of the molecule is perturbated owing to the hydroxy and epoxy groups on its surface, which resulted in the bent geometry (Fig. 3b). The map of electrostatic potential was calculated at the outer contour of electron density (isoval = 0.0004; mapped with ESP; Fig. 3c). It can be noticed that the H-atoms of -OH and -$CONH_2$ groups are positively charged, while the oxygen atoms of -COOH, -$CONH_2$, -OH, and epoxy groups are negative or slightly negatively charged.

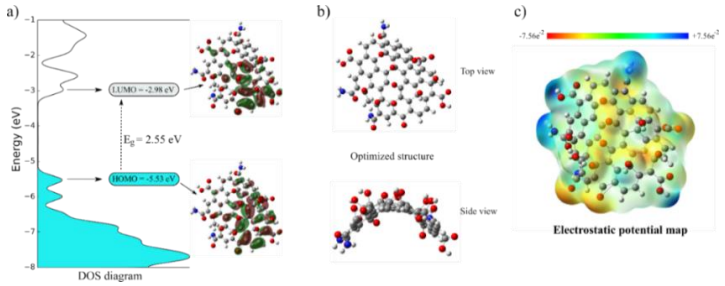

Fig. 3. a) Total density of state diagram (TDOS) of N-doped GQDs, b) the optimized structure of GQD's cluster (two views), and c) electrostatic potential map (ESP) as calculated at B3LYP/6-31G(d,p) level of theory.

To estimate the adsorption of Pd(II) ions at the GQD surface, we selected four sites of the GQDs molecule. The relative Gibbs free energy of adsorption in aqueous solution (ΔG_{sol}) was calculated as the difference between Pd/GQD adsorbed system and isolated Pd(II) ions plus free GQD molecule, based on frequency analysis upon the structure optimizations. Therefore, a negative value of ΔG_{sol} indicates that the adsorption process is energetically favorable. The strongest binding was calculated for the conformation in which the Pd(II) ion is coordinated to the deprotonated -COO^- group (ΔG_{sol} = -1.72 eV), while the weakest binding refers to the geometry where Pd(II) is located above one of the C_6-rings (ΔG_{sol} = -0.80 eV). Surprisingly, high adsorption energy was calculated for the geometry with Pd(II)-ion coordinated to the C=C double bond (Fig. 4a). The NBO charges of adsorbed Pd ions follow the order of Gibbs free energy changes: the higher positive charge on Pd indicates more negative ΔG_{sol} values and stronger adsorption (Fig. 4b).

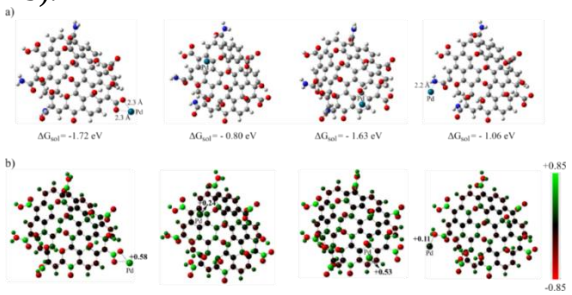

Fig. 4. a) The four optimized GQD structures in which Pd(II) ions are adsorbed to the molecule's different parts. b) The calculated NBO charges of four structures are presented in the same charge range and color scheme.

The geometry optimization of the GQD···CF system resulted in a structure with a bifurcated hydrogen-bond with respective -COO···H_2N- distances of 2.10 and 2.77 Å (Fig. 5a). The calculated ΔG_{sol} value is -0.12 eV (-2.76 kcal/mol), which is within the typical range of H-bond strengths. On the other hand, the ESC map of this adduct reveals that a highly negative region is associated with -COO···H_2N- interacting fragments of GQD and CF molecules, respectively (Fig. 5b).

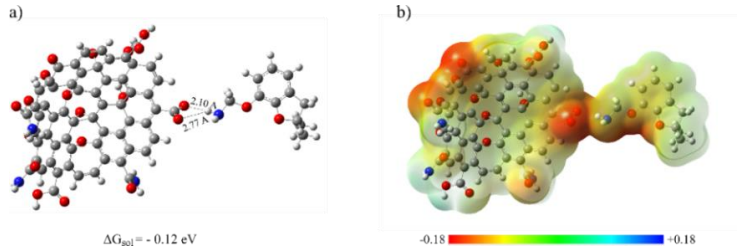

Fig. 5. a) The optimized GQD ⋯ CF structure with assigned hydrogen bonds and b) electrostatic potential map (ESC) as calculated at B3LYP/6-31G(d,p) level of theory.

Conclusion

In summary, we successfully resolved Pd(II) and CF-induced mechanism of PL change of irradiated amino/amide doped GQDs and Pd(II) using FTIR spectroscopy and DFT analysis. DFT analysis represents a promising, fast, and efficient method in the investigation of intermolecular interactions without additional consumption of chemicals.

Acknowledgements

This work was financially supported by the Ministry of Education, Science and Technological Development of the Republic of Serbia (Grant No. 451-03-9/2022-14/200017).

References

[1] S. Dorontic, A. Bonasera, M. Scopelliti, M. Mojsin, M. Stevanovic, O. Markovic, S. Jovanovic, Journal of Luminescence, 252 (2022) 119311.
[2] S. Dorontic, A. Bonasera, M. Scopelliti, O. Markovic, D. Bajuk Bogdanović, G. Ciasca, S. Romanò, I. Dimkić, M. Budimir, D. Marinković, S. Jovanovic, Nanomaterials, 12 (2022).
[3] https://archive.epa.gov/pesticides/reregistration/web/html/carbofuran_ired_fs.html.
[4] S. Dorontić, S. Jovanović, A. Bonasera, Materials, 14 (2021).
[5] S. Jovanovic, A. Bonasera, S. Dorontic, D. Zmejkoski, D. Milivojevic, T. Janakiev, B. Todorovic Markovic, Materials2022.
[6] S. Jovanović, S. Dorontić, D. Jovanović, G. Ciasca, M. Budimir, A. Bonasera, M. Scopelliti, O. Marković, B. Todorović Marković, Ceramics International, 46 (2020) 23611-23622.
[7] M.J.T. Frisch, G. W.; Schlegel, H. B.; Scuseria, G. E.; Robb, M. A.; Cheeseman, J. R.; Scalmani, G.; Barone, V.; Mennucci, B.; Petersson, G. A.; et al. Gaussian 09, Revision D.01; Gaussian, Inc.: Wallingford, CT, USA, 2009.
[8] A.V. Marenich, C.J. Cramer, D.G. Truhlar, The Journal of Physical Chemistry B, 113 (2009) 6378-6396.
[9] A.D. Becke, The Journal of Chemical Physics, 98 (1993) 5648-5652.
[10] C. Lee, W. Yang, R.G. Parr, Physical review. B, Condensed matter, 37 (1988) 785-789.
[11] P.J. Hay, W.R. Wadt, The Journal of Chemical Physics, 82 (1985) 299-310.
[12] R. Ditchfield, W.J. Hehre, J.A. Pople, Journal of Chemical Physics, 54 (1971) 724-728.
[13] A.N. Frisch, A. B.; Holder, A. J. Gauss View Molecular Visualization Program; User Manual: Pittsburg, CA, USA, 2001.
[14] N.M. O'Boyle, A.L. Tenderholt, K.M. Langner, Journal of Computational Chemistry, 29 (2008) 839-845.